Annals of
SURGICAL ONCOLOGY
OFFICIAL JOURNAL OF THE SOCIETY OF SURGICAL ONCOLOGY

CrossMark

ORIGINAL ARTICLE – BREAST ONCOLOGY

Correlation Between F-18 Fluorodeoxyglucose Positron Emission Tomography Metabolic Parameters and Dynamic Contrast-Enhanced MRI-Derived Perfusion Data in Patients with Invasive Ductal Breast Carcinoma

Tae Hee Kim, MD, PhD[1], Joon-Kee Yoon, MD, PhD[2], Doo Kyoung Kang, MD[1], Su Jin Lee, MD, PhD[2], Yong Sik Jung, MD[3], Hyunee Yim, MD, PhD[4], and Young-Sil An, MD, PhD[2]

[1]Department of Radiology, Ajou University School of Medicine, Suwon, Korea; [2]Department of Nuclear Medicine and Molecular Imaging, School of Medicine, Ajou University School of Medicine, Suwon, Korea; [3]Department of Surgery, Ajou University School of Medicine, Suwon, Korea; [4]Department of Pathology, Ajou University School of Medicine, Suwon, Korea

ABSTRACT

Purpose. The aim of this study was to establish possible relationships among the metabolic and vascular characteristics of breast cancer using dynamic contrast-enhanced magnetic resonance imaging (DCE-MRI) and F-18 fluorodeoxyglucose (FDG) positron emission tomography/computed tomography (PET/CT) imaging.

Methods. Sixty-seven female patients with invasive ductal breast carcinoma (age 32–79 years) who underwent FDG PET/CT and DCE–MRI prior to cancer treatment were included in the study. The maximum standardized uptake value (SUV_{max}), metabolic tumor volume, total lesion glycolysis (TLG), and heterogeneity factor (HF) were derived from FDG PET/CT. The DCE–MRI parameters K_{trans}, K_{ep}, and V_e were obtained for all tumors, and relationships between the metabolic and perfusion parameters were sought via Spearman's rank correlation analysis. The prognostic significance of clinicopathological and imaging parameters in terms of recurrence-free survival (RFS) was also evaluated.

Results. No significant correlation between perfusion and metabolic parameters ($p > 0.05$) was found, except between SUV_{max} and V_e ($p = 0.001$, rho $= -0.391$). Recurrence developed in 12 of the 67 patients (17.9 %, follow-up period 8–41 months). Age ($p = 0.016$) and HF ($p = 0.027$) were significant independent predictors of recurrence-free survival (RFS) upon multivariate analysis. The RFS of patients under 40 years of age was significantly poorer than that of older patients ($p < 0.001$). Survival of patients with more heterogeneous tumors (HF less than -0.12) was poorer than those with relatively homogenous tumors ($p = 0.033$).

Conclusions. Tumors with higher levels of glucose metabolism (SUV_{max} values) exhibited higher tumor cellularities (V_e values). Also, of the various metabolic and perfusion parameters available, tumor heterogeneity measured via FDG PET/CT (HF) may be useful in predicting RFS in breast cancer patients.

F-18 fluorodeoxyglucose (FDG) positron emission tomography/computed tomography (PET/CT) and dynamic contrast-enhanced magnetic resonance imaging (DCE-MRI) measure functional properties (metabolic and perfusion data, respectively), and are valuable in the assessment of breast cancer.[1,2]

The most frequently derived parameters from FDG PET are the standardized uptake value (SUV), and volumetric metabolic parameters (including the metabolic tumor volume [MTV] and total lesion glycolysis [TLG]).[3–5] Furthermore, intratumoral metabolic heterogeneity, assessed via FDG PET imaging, has recently been shown to be a useful parameter in the evaluation of various tumors, including breast cancer.[6–8]

DCE-MRI data reflect tumor perfusion; the technique assesses the density, integrity, and leakiness of tissue vasculature. Most quantitative approaches measure three

perfusion parameters, i.e. the forward volume transfer constant (K_{trans}, min^{-1}), the rate constant for the escape of contrast agent from the extracellular extravascular space into the plasma compartment (K_{ep}, min^{-1}); and the fractional volume of the extravascular extracellular space (V_{e}).[9,10]

The definition of relationships among such functional parameters would facilitate our understanding of tumor characteristics and widen the clinical utilities of the parameters in oncology generally. It is usually assumed that glucose metabolism and the extent of perfusion are significantly related. However, MRI evaluation of contrast, and FDG uptake, explore entirely different physiological mechanisms, which thus may not be necessarily associated. Earlier small-scale studies sought relationships between metabolic and perfusion data (derived using MRI and FDG PET, respectively) in breast lesions,[11,12] but the results were not consistent.

Based on these considerations, we retrospectively sought relationships between FDG PET/CT-derived parameters and DCE-MRI-based parameters. In addition, we sought to determine whether any measured parameter predicted recurrence-free survival (RFS) in patients with invasive ductal breast carcinoma.

METHODS

Patients

We studied 67 females (median age 46 years, range 32–79 years) with invasive ductal breast carcinoma treated at a single institution (Ajou University Hospital, Suwon, Korea). All patients underwent both DCE-MRI and FDG PET/CT prior to any treatment. No patient had diabetes mellitus or a blood glucose level over 150 mg/dL prior to FDG PET/CT; image quality was thus not adversely affected. The number of days that elapsed between MRI and PET ranged from 0 to 9 (median 2 days). Patient characteristics, including age, histology, stage, and treatment modalities, were obtained via chart review performed by an independent reviewer blinded to MRI and PET results. Clinical stage was determined using the criteria of the American Joint Committee on Cancer (AJCC), 6th edition.[13] Tumor size was assessed by MRI imaging. After staging, 64 patients (95.5 %) underwent surgical treatment, and neoadjuvant chemotherapy was prescribed for 23 patients prior to surgery. Adjuvant chemotherapy and/or radiation therapy were followed by surgery. The remaining three patients with advanced-stage disease underwent chemotherapy and radiation therapy without surgery. Clinical follow-up was performed every 6 months; the median follow-up duration was 36 months (range 8–41 months). Patient characteristics are summarized in Table 1.

TABLE 1 Patient characteristics

| Demographic	N
Age [years; median (range)]	46 (37–79)
Female sex (%)	67 (100)
Histopathology (%)	
Invasive ductal carcinoma	67 (100)
Tumor size [mm; median (range)]	22 (10–120)
T stage (%)	
T1	27 (40.3)
T2	33 (49.3)
T3	5 (7.5)
T4	2 (2.9)
AJCC stage (%)	
I	17 (25.3)
II	40 (59.8)
III	9 (13.4)
IV	1 (1.5)
Treatment (%)	
Neoadjuvant chemotherapy + surgery + chemotherapy or/and radiation therapy	23 (34.3)
Surgery + chemotherapy or/and radiation therapy	41 (61.2)
Chemotherapy and radiation therapy without surgery	3 (4.5)

AJCC American Joint Committee on Cancer

The clinical design of this retrospective study was approved by the Institutional Review Board of Ajou University (MED-MDB-14-268), with waiver of any need for informed consent.

F-18 Fluorodeoxyglucose (FDG) Positron Emission Tomography/Computed Tomography (PET/CT) Protocol

After fasting for at least 6 h, each patient received 5 MBq/kg of FDG intravenously. The blood glucose level at the time of injection was <150 mg/dL in all patients. Patients were instructed to rest comfortably for 60 min and to urinate prior to scanning. Whole-body PET/CT images were obtained using a Discovery ST scanner (GE Healthcare, Milwaukee, WI, USA). Seven to eight frames (3 min/frame) of emission PET data were acquired in the three-dimensional (3D) mode after obtaining a non-contrast CT scan from the base of the skull to the upper thigh (120 kV; 30–100 mA in the AutomA mode; section width = 3.75 mm). Emission PET images were reconstructed using an iterative method (ordered-subsets expectation maximization with two iterations and 20 subsets, field of view = 600 mm, slice thickness = 3.27 mm) and attenuation-corrected by reference to the non-contrast CT image.

FIG. 1 **a** Representative PET images from left-breast cancer patients using several SUV thresholds from 40 to 80 %. Metabolic tumor volumes fell as the SUV_{max} threshold increased. **b** MTV-threshold curve obtained plotting MTVs and threshold calculated at 40, 50, 60, 70, and 80 % of SUV_{max}. The heterogeneity factor (−0.35) is the slope of the linear regression equation. *MTV* metabolic tumor volume, *PET* positron emission tomography, *SUV* standardized uptake value, SUV_{max} maximum SUV

A

Threshold 40%   Threshold 60%   Threshold 80%

B

$y = -0.35x + 31.61$

Metabolic tumor volume(cm³)

Threshold (% of SUVmax)
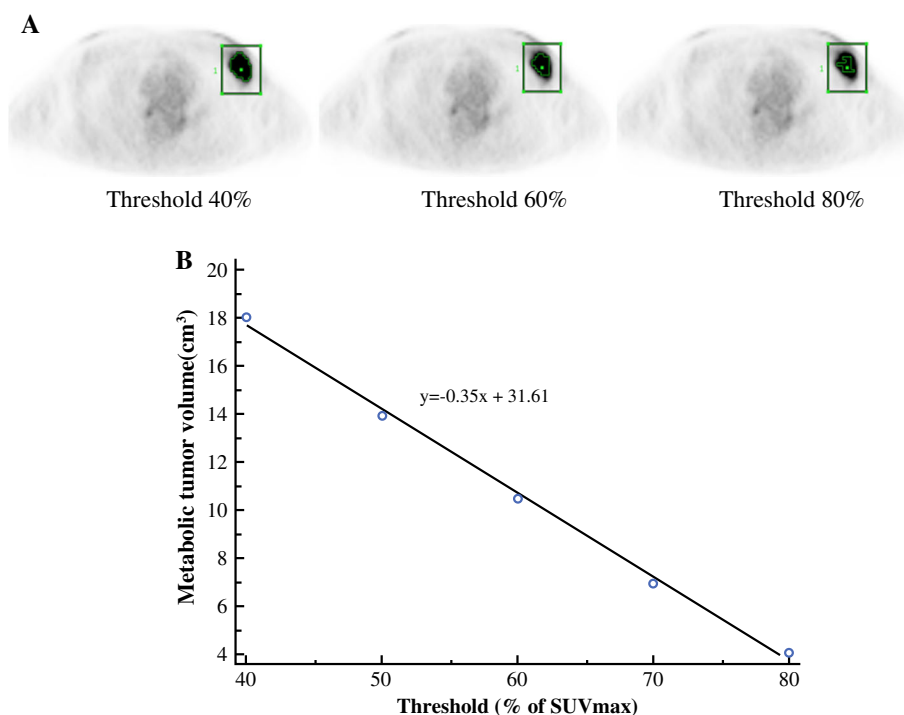
Magnetic Resonance Imaging Protocol

All MR examinations were performed using a 1.5-T system (Signa HDxt; GE Medical Systems) fitted with a dedicated breast coil (an eight-channel HD breast array, GE Medical Systems).

Fat-suppressed, T2-weighted, fast spin-echo sagittal images were first obtained. The following imaging parameters were used: flip angle 90°, image matrix 320 × 256, field of view 320 × 320 mm, section thickness 3.0 mm, and section gap 0 mm. For baseline T1 calculations, pre-contrast transverse 3D gradient-echo images were obtained using flip angles of 3° and 12° and the following parameters: TR/TE = 3.62/1.78 ms, field of view = 280 mm, matrix 200 × 200, number of slices = 40, slice thickness = 2 mm (interpolated), no gap, and receiver bandwidth = 50 kHz. DCE-MRIs were obtained using a 3D fast spoiled gradient-echo (SPGR) sequence featuring parallel imaging acceleration, through the entire breast, employing a flip angle of 20° and the other parameters used to obtain pre-contrast images. We acquired a total of 42 phases of non-fat-saturated T1-weighted images before and after administration of gadolinium with temporal resolution of 11 s. Scan time was 7 min and 42 s. Gadobutrol (Gadovist; Bayer Schering Pharma, Berlin, Germany) was injected into an antecubital vein at a dose of 0.1 mmol/kg of body weight and at a rate of 3 mL/s, followed by a 20-mL saline flush.

Image Analysis

A nuclear medicine specialist with 10 years of PET experience reviewed all FDG PET/CT images on a dedicated workstation (GE Advantage Workstation 4.4). Volumetric metabolic parameters were obtained using the Volume Viewer software. The volumetric region of interest (VOI) was carefully placed over the breast lesion exhibiting elevated FDG activity, compared with normal tissue, to avoid overlap with adjacent FDG-avid structures and areas exhibiting physiological uptake. A threshold of 50 % SUV_{max} was used to delineate the MTV. All SUVs were estimated based on injected dose and body weight, and the SUV_{max}, mean SUV (SUV_{mean}), and MTV of each lesion were calculated automatically. TLG was calculated by multiplying the SUV_{mean} by the MTV. We acquired an additional metabolic parameter, the heterogeneity factor (HF), which reflects the intratumoral heterogeneity of FDG uptake. HF was defined as the derivative (dV/dT) of the MTV-threshold function calculated using a series of SUV thresholds (from 40 to 80 %) of each primary tumor. Figure 1a shows representative PET images obtained using various SUV thresholds. The MTVs at each threshold were recorded, and the HF was next calculated as the slope of the linear regression on the MTV-threshold curve (Fig. 1b). Thus, HF was negative, and a larger absolute HF value with lower HF reflected more heterogenous tumors. This method was adapted from a published PET analysis protocol.[14]

TABLE 2 Correlations between metabolic and perfusion parameters

	K_{trans} 0.26 (0.06–1.86)[a]	K_{ep} 0.66 (0.23–2.76)[a]	V_e 0.41 (0.17–0.98)[a]
SUV$_{max}$	$p = 0.209$	$p = 0.218$	$p = 0.001$[†]
6.10 (1.30–21.00)[a]	(rho = −0.155)	(rho = 0.152)	(rho = −0.391)
MTV	$p = 0.578$	$p = 0.909$	$p = 0.506$
2.73 (0.65–57.19)[a]	(rho = 0.069)	(rho = −0.014)	(rho = 0.083)
TLG	$p = 0.886$	$p = 0.939$	$p = 0.195$
14.10 (1.96–388.89)[a]	(rho = −0.018)	(rho = 0.106)	(rho = −0.160)
HF	$p = 0.784$	$p = 0.553$	$p = 0.434$
−0.08 (−2.36 to −0.02)[a]	(rho = −0.034)	(rho = 0.074)	(rho = −0.097)

HF heterogeneity factor, *MTV* metabolic tumor volume, *SUV$_{max}$* maximum standardized uptake value, *TLG* total lesion glycolysis

[†] $p < 0.05$

[a] Median (range)

To analyze DCE-MRI data, ViaPack software (GE Medical Systems) was used. The arterial input function (AIF) was measured in the aortic arch, or at the highest level of the scanned aorta if the aortic arch was not scanned. Several ROIs for AIF were positioned in the center of the aortic lumen, and the ROI showing the highest maximal peak enhancement and the fastest peak arrival time was considered to reflect the AIF. To measure tumor perfusion parameters, ROIs were drawn manually around the tumor margins of three consecutive axial sections that included the center of the tumor mass. Care was taken to exclude adjacent soft tissues and blood vessels. Perfusion parameters, including K_{trans}, K_{ep}, and V_e, were calculated pixelwise over the entire region, and the mean values of parameters within ROIs were automatically calculated and displayed. We used the highest mean values in calculations. All MR images were reviewed in consensus by two radiologists with 4 and 8 years of experience in interpreting breast imaging. The enhancement kinetics of each pixel were measured throughout the entire scan time and adapted to two-compartment models, as described by Tofts et al.[10,15]

Histopathological Evaluation

Surgical specimens from macroscopic tumor areas were serially sliced at 5-mm intervals, and paraffin-embedded sections were prepared and stained with hematoxylin and eosin. The specimens were evaluated in terms of the following histopathological features: histological carcinoma type, Black nuclear grade (1 = poorly differentiated, 2 = moderately differentiated, and 3 = well-differentiated), and modified Bloom–Richardson histological grade (1 = well-differentiated, 2 = moderately differentiated,

and 3 = poorly differentiated). Expression of estrogen receptor (ER), progesterone receptor (PR), and human epidermal growth factor receptor 2 (HER2) were evaluated using standard immunohistochemical staining methods featuring formation of avidin–biotin complexes. All primary antibodies were monoclonal: anti-ER (Dako Corporation, Carpinteria, CA, USA; 1:50); anti-PR (Dako Corporation; 1:50); and anti-c-erbB2 (Novocastra Laboratories Ltd, Newcastle-Upon-Tyne, UK; 1:200). ER and PR positivity were considered present when 1 % or more of nuclei stained positively at ×10 magnification. The intensity of c-erbB-2 staining was scored as 0, 1+, 2+, or 3+. Tumors with 3+ scores were classified as HER2-positive, and tumors with 0 or 1+ scores were classified as negative. In tumors with 2+ scores, gene amplification via fluorescence in situ hybridization was used to determine HER2 status. All specimens were reviewed by a pathologist with 16 years of experience.

Statistical Analysis

Correlations between perfusion and metabolic parameters were sought using Spearman's rank test. RFS was used to measure clinical outcomes, and was defined as the period from initial diagnosis to recurrence. Locoregional recurrence, distant recurrence, and death from any cause were considered to be relevant events.[16] To assess the prognostic significance of clinicopathological and imaging parameters, we performed both univariate and multivariate analyses using Cox's proportional hazards regression model. Survival functions were estimated using the Kaplan–Meier method and compared using the log-rank test. We selected the cut-off value maximizing the profile partial likelihood upon Cox's regression, using a binary

TABLE 3 Univariate analysis of factors influencing recurrence-free survival using Cox's proportional hazards regression model

Covariate	p value	HR	95 % CI
Age	<0.001*	0.85	0.77–0.95
Tumor size	0.024*	1.26	1.07–1.48
AJCC stage (I, II vs. III, IV)	0.031*	4.42	1.33–14.75
Treatment (neoadjuvant chemotherapy + surgery + chemotherapy and/or radiation therapy vs. surgery + chemotherapy and/or radiation therapy vs. chemotherapy and radiation therapy without surgery)	0.052	0.25	0.07–0.84
Nuclear grade (grade 1 vs. grades 2, 3)	0.001*	1.51	3.24 –7.04
Histological grade (grades 1, 2 vs. grade 3)	0.104	3.30	0.69–15.73
ER (negative vs. positive)	0.462	0.65	0.21–2.01
PR (negative vs. positive)	0.160	0.44	0.14–1.39
HER2 (negative vs. positive)	0.806	0.85	0.23–3.12
SUV_{max}	0.201	1.08	0.97–1.21
Metabolic tumor volume	0.009*	1.07	1.03–1.11
Total lesion glycolysis	0.002*	0.96	0.93–0.98
Heterogeneity factor	0.007*	1.01	1.01–1.02
K_{trans}	0.829	1.19	0.27–5.27
K_{ep}	0.958	1.04	0.31–3.44
V_e	0.357	3.34	0.28–40.12

AJCC American Joint Committee on Cancer, *CI* confidence interval, *ER* estrogen receptor, *HER2* human epidermal growth factor receptor 2, *HR* hazard ratio, *PR* progesterone receptor, SUV_{max} maximum standardized uptake value

* $p < 0.05$

explanatory variable. MedCalc (MedCalc Software bvba, version 14.8.1, Ostend, Belgium) was used in all statistical analyses. p values <0.05 were considered to indicate statistical significance.

RESULTS

There was No Significant Correlation Between Perfusion and Metabolic Parameters, Except Between SUV_{max} and V_e

SUV_{max} was significantly (negatively) correlated with V_e; the rho values ranged from −0.577 to −0.166 ($p < 0.001$, rho = −0.391) (Table 2). No significant relationship was evident between any other perfusion and metabolic parameters (Table 2).

Tumor Heterogeneity Measured Via FDG PET/CT May be Useful in Predicting Prognosis in Breast Cancer Patients

Twelve patients (12/67, 17.9 %) developed recurrences during follow-up. Locoregional recurrence occurred in four patients, distant recurrence in six patients, and two patients died. Upon univariate analysis, age, tumor size, AJCC stage, nuclear grade, and volumetric metabolic parameters (MTV, TLG, and HF) were all significant prognostic factors for

RFS (all p values <0.05). The MRI perfusion parameters did not include any significant prognostic factor. The results of univariate analysis are summarized in Table 3. Multivariate analysis showed that only age ($p < 0.001$; hazard ratio [HR] 0.85; 95 % confidence interval [CI] 0.74–0.97) and HF ($p = 0.027$; HR 1.01, 95 % CI 1.00–1.02) were independent prognostic parameters for RFS.

Kaplan–Meier comparisons of age and HF are shown in Fig. 2. Survival differed significantly between younger and older patients (cut-off, 40 years) (Fig. 2a). Survival of the low-HF group (HF less than −0.12) with more heterogenous tumors was poorer than that of the high-HF group with relatively homogenous tumors (Fig. 2b).

DISCUSSION

To our knowledge, this is the first study to try to establish relationships between metabolic and perfusion parameters, in an effort to identify factors that could serve to optimally predict RFS in homogeneous populations of patients with invasive ductal breast carcinoma.

We found no significant correlation between any metabolic and perfusion parameter of breast tumors, except for SUV_{max} and V_e. Gadolinium chelate (the MRI contrast material) is distributed principally in the interstitial space because the material does not cross cell membranes. Therefore, the volume of the extracellular–extravascular
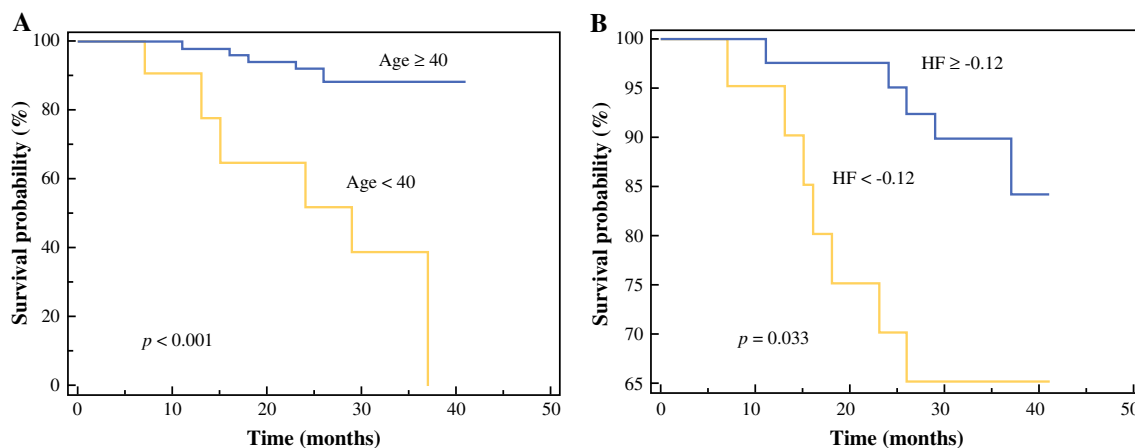
FIG. 2 Kaplan–Meier estimates of RFS by age and HF. **a** Those aged less than 40 years showed significantly poorer prognoses than older patients ($p < 0.001$; HR 9.04; 95 % CI 1.37–59.78). **b** The prognoses of patients with more heterogeneous tumors (HF less than −0.12) was poorer than those with relatively homogenous tumors ($p = 0.033$; HR 3.23; 95 % CI 0.94–11.09). *CI* confidence interval, *HF* heterogeneity factor, *HR* hazard ratio

space per unit volume of tissue (V_e), which depends on endothelial factors and the interstitial environment, reflects tumor cellularity; a lower V_e indicates higher cellularity.[17] Thus, the negative correlation evident between SUV_{max} and V_e indicated that breast tumors exhibiting higher-level glucose metabolism tended to be of greater cellularity. A significant correlation between tumor cellularity, as revealed by pathology, and SUV was found in a previous study,[18] but our current work is the first to report a correlation between tumor cellularity as revealed by MRI (V_e) and SUV_{max}. However, neither K_{trans} nor K_{ep} exhibited a significant relationship with glucose metabolism. K_{trans} reflects a combination of microvascular blood flow, and vessel permeability and density;[10] K_{ep} reflects permeability only, being unaffected by blood flow.[19] Therefore, our results suggest that tumor vascular characteristics were not associated with metabolic factors, consistent with data of a previous study by Brix et al.[12], which found no correlation between any MRI pharmacokinetic parameter and SUV derived via FDG PET imaging. This is difficult to explain. Obviously, tumor vasculature (measured by blood flow) and vessel permeability play important roles in intracellular FDG uptake. The absence of any observed relationship between these parameters may be because the late phase of FDG uptake features principally glucose utilization and intracellular trapping of the phosphorylated form of FDG. Thus, tumor metabolic activity may be high, even if blood flow and vascular permeability are limited.[12]

Our multivariate analysis featuring adjustment for several variables revealed that age and intratumoral metabolic heterogeneity independently predicted RFS in breast cancer patients. It is well known that breast cancer in the young exhibits aggressive features associated with poor prognoses[20] but, to our knowledge, this is the first report to show that tumor heterogeneity measured via FDG PET predicts survival of breast cancer patients. Only a single prior study found that tumor heterogeneity (as revealed by textural analysis) was a pathologically prognostic factor in such patients.[21] Intratumoral heterogeneity measured via FDG PET/CT is becoming more popular, and affords new insights into the tumor characteristics of various cancers.[22,23] Tumor heterogeneity may be caused by necrosis and hypoxia, and is associated with enhanced tumor aggressiveness and poorer prognosis in patients with many types of malignancies.[24–26] We obtained HFs using the derivatives (dV/dT values) of the lesional MTV-threshold functions, as in a previous study.[14] We prefer this method to textural analysis. The former method is convenient, and better suited to clinical practice, than the latter method (featuring mathematical quantification of intensity differences between contiguous pixels on digital images).[27]

Our study had several limitations. We present RFS but not overall survival data because our follow-up periods were relatively short (8–41 months); it would be more clinically meaningful to measure 5-year survival rates. Continuation of our study will identify parameters predictive of overall survival. The other limitation is that we could not evaluate the change of imaging parameters in patients undergoing chemotherapy or radiation therapy. The effects of drugs and radiation effects would be expected to depend on tumor vascular and metabolic characteristics. Therefore, monitoring changes in flow and metabolic parameters during therapy would better predict treatment responses. Notably, the numbers of breast cancer patients receiving neoadjuvant chemotherapy are currently increasing, and identification of perfusion/metabolic parameters predicting responses after neoadjuvant chemotherapy must be performed in future.

CONCLUSIONS

No significant association between any vascular and metabolic parameter of the lesions of invasive ductal breast carcinoma were found, except between glucose metabolism (SUV_{max}) and tumor cellularity measured via DCE-MRI (V_e). Also, of the various metabolic and perfusion parameters, tumor heterogeneity measured via FDG PET/CT may be useful in predicting RFS in breast cancer patients.

REFERENCES

1. Peters NH, Borel Rinkes IH, Zuithoff NP, Mali WP, Moons KG, Peeters PH. Meta-analysis of MR imaging in the diagnosis of breast lesions. *Radiology*. 2008;246:116–24.
2. Groheux D, Espie M, Giacchetti S, Hindie E. Performance of FDG PET/CT in the clinical management of breast cancer. *Radiology*. 2013;266:388–405.
3. Tateishi U, Gamez C, Dawood S, Yeung HW, Cristofanilli M, Macapinlac HA. Bone metastases in patients with metastatic breast cancer: morphologic and metabolic monitoring of response to systemic therapy with integrated PET/CT. *Radiology*. 2008;247:189–96.
4. Lee HY, Hyun SH, Lee KS, et al. Volume-based parameter of 18)F-FDG PET/CT in malignant pleural mesothelioma: prediction of therapeutic response and prognostic implications. *Ann Surg Oncol*. 2010;17:2787–94.
5. Guillem JG, Moore HG, Akhurst T, et al. Sequential preoperative fluorodeoxyglucose-positron emission tomography assessment of response to preoperative chemoradiation: a means for determining longterm outcomes of rectal cancer. *J Am Coll Surg*. 2004;199:1–7.
6. van Baardwijk A, Bosmans G, van Suylen RJ et al. Correlation of intra-tumour heterogeneity on 18F-FDG PET with pathologic features in non-small cell lung cancer: a feasibility study. *Radiother Oncol*. 2008;87:55–8.
7. Kidd EA, Grigsby PW. Intratumoral metabolic heterogeneity of cervical cancer. *Clin Cancer Res*. 2008;14:5236–41.
8. Tixier F, Groves AM, Goh V, et al. Correlation of intra-tumor 18F-FDG uptake heterogeneity indices with perfusion CT derived parameters in colorectal cancer. *PLoS One*. 2014;9:e99567.
9. Yankeelov TE, Gore JC. Dynamic contrast enhanced magnetic resonance imaging in oncology: theory, data acquisition, analysis, and examples. *Curr Med Imaging Rev*. 2009;3:91–107.
10. Tofts PS, Brix G, Buckley DL, et al. Estimating kinetic parameters from dynamic contrast-enhanced T(1)-weighted MRI of a diffusable tracer: standardized quantities and symbols. *J Magn Reson Imaging*. 1999;10:223–32.
11. Semple SI, Gilbert FJ, Redpath TW, et al. The relationship between vascular and metabolic characteristics of primary breast tumours. *Eur Radiol*. 2004;14:2038–45.
12. Brix G, Henze M, Knopp MV, et al. Comparison of pharmacokinetic MRI and [18F] fluorodeoxyglucose PET in the diagnosis of breast cancer: initial experience. *Eur Radiol*. 2001;11:2058–70.
13. Singletary SE, Allred C, Ashley P, et al. Revision of the American Joint Committee on Cancer staging system for breast cancer. *J Clin Oncol*. 2002;20:3628–36.
14. Huang B, Chan T, Kwong DL, Chan WK, Khong PL. Nasopharyngeal carcinoma: investigation of intratumoral heterogeneity with FDG PET/CT. *AJR Am J Roentgenol*. 2012;199:169–74.
15. Tofts PS. Modeling tracer kinetics in dynamic Gd-DTPA MR imaging. *J Magn Reson Imaging*. 1997;7:91–101.
16. Hudis CA, Barlow WE, Costantino JP, et al. Proposal for standardized definitions for efficacy end points in adjuvant breast cancer trials: the STEEP system. *J Clin Oncol*. 2007;25:2127–32.
17. Knopp MV, von Tengg-Kobligk H, Choyke PL. Functional magnetic resonance imaging in oncology for diagnosis and therapy monitoring. *Mol Cancer Ther*. 2003;2:419–26.
18. Higashi T, Tamaki N, Torizuka T, et al. FDG uptake, GLUT-1 glucose transporter and cellularity in human pancreatic tumors. *J Nucl Med*. 1998;39:1727–35.
19. Miller JC, Pien HH, Sahani D, Sorensen AG, Thrall JH. Imaging angiogenesis: applications and potential for drug development. *J Natl Cancer Inst*. 2005;97:172–87.
20. Assi HA, Khoury KE, Dbouk H, Khalil LE, Mouhieddine TH, El Saghir NS. Epidemiology and prognosis of breast cancer in young women. *J Thorac Dis*. 2013;5 Suppl 1:S2–8.
21. Soussan M, Orlhac F, Boubaya M, et al. Relationship between tumor heterogeneity measured on FDG-PET/CT and pathological prognostic factors in invasive breast cancer. *PLoS One*. 2014;9:e94017.
22. Cook GJ, Yip C, Siddique M, et al. Are pretreatment 18F-FDG PET tumor textural features in non-small cell lung cancer associated with response and survival after chemoradiotherapy? *J Nucl Med*. 2013;54:19–26.
23. Tixier F, Le Rest CC, Hatt M, et al. Intratumor heterogeneity characterized by textural features on baseline 18F-FDG PET images predicts response to concomitant radiochemotherapy in esophageal cancer. *J Nucl Med*. 2011;52:369–78.
24. Lu X, Kang Y. Hypoxia and hypoxia-inducible factors: master regulators of metastasis. *Clin Cancer Res*. 2010;16:5928–35.
25. Leek RD, Landers RJ, Harris AL, Lewis CE. Necrosis correlates with high vascular density and focal macrophage infiltration in invasive carcinoma of the breast. *Br J Cancer*. 1999;79:991–5.
26. Jimenez RE, Wallis T, Visscher DW. Centrally necrotizing carcinomas of the breast: a distinct histologic subtype with aggressive clinical behavior. *Am J Surg Pathol*. 2001;25:331–7.
27. Chicklore S, Goh V, Siddique M, Roy A, Marsden PK, Cook GJ. Quantifying tumour heterogeneity in 18F-FDG PET/CT imaging by texture analysis. *Eur J Nucl Med Mol Imaging*. 2013;40:133–40.